Microreactors

Nanocapillary Arrays Effect Mixing and Reaction in Multilayer Fluidic Structures**

Tzu-C. Kuo, Hee-K. Kim, Donald M. Cannon, Jr., Mark A. Shannon, Jonathan V. Sweedler, and Paul W. Bohn**

Chemical and biochemical manipulations carried out in integrated devices have generated considerable interest in total-analysis microsystems (μTAS)[1,2] and in micrometer-scale laboratory chemical manipulations.[3–6] Microfluidics enable significant reductions in sample size. However, the low Reynolds numbers can lead to laminar flow.[4] Mixing, a

[*] Dr. T.-C. Kuo, H.-K. Kim, Dr. D. M. Cannon, Jr., Prof. M. A. Shannon, Prof. J. V. Sweedler, Prof. P. W. Bohn
Department of Chemistry
Department of Mechanical and Industrial Engineering, and
Beckman Institute for Advanced Science and Technology
University of Illinois at Urbana-Champaign
600 South Mathews Ave., Urbana, IL 61801 (USA)
Fax: (+1) 217-244-8068
E-mail: sweedler@scs.uiuc.edu
bohn@scs.uiuc.edu

[**] This work was supported by DARPA under grant F30602-00-2-0567, the Department of Energy under grants DE FG02 88ER13949 and DE FG02 99ER62797 and the National Institutes of Allergies and Infectious Diseases under the Great Lakes Regional Center for Excellence. The authors thank G. Fried and K. Garsha for assistance with confocal microscopy and for discussions.

Supporting information for this article is available on the WWW under http://www.angewandte.org or from the author.

  DOI: 10.1002/ange.200353279

basic requirement for reactions in solution, between parallel laminar streams depends on diffusion, which, except in special geometries,[7,8] may be too slow. To decrease the mixing times, workers have exploited moving parts, external forces, or changes in channel geometry to achieve both active (vortex chambers[9] and microstirrers,[10,11] sinusoidally alternating electric fields[12,13] and ultrasonic vibration[14]) and passive (alternating microchannel geometry or complex channel networks) mixing.[15] Electrokinetic mixing has been demonstrated,[16] and chaotic flow can be induced, with oriented ridges, serpentine 3D channel structures,[17] microplume arrays[18] and microbead-packed channels,[19] which generate efficient mixing by reducing the effective thickness of fluid laminae.

Herein we report an alternative that opens the possibility of rapid mixing and reaction in the important class of 3D fluidic architectures.[20–25] Mixing is implemented in structures with characteristic length scales of nanometers, such that diffusive transport occurs on experimentally convenient millisecond timescales; mixing occurs within micron distances rather than the centimeters that are often needed for laminar microflows. To illustrate the advantages of nanoscale features, consider two parallel fluid streams, separated by 500 nm, injected into a solution that contains a complementary reactant. With a diffusion coefficient of $5\times10^{-7}\,cm^2s^{-1}$ linear diffusion mixes the reactants in only 2.5 ms. This arrangement is implemented by nanocapillary membranes with monodisperse distributions of nanometer diameter channels, which are used to control molecular transport in multilevel microfluidic systems.[21,23–25] Typically, these membranes contain about 3×10^4 nanopores in $100\times100\,\mu m^2$, that is, the mean interpore separation is about 580 nm. Because fluid is transferred under electrokinetic control at appreciable velocity ($v_{max}\approx2.5\,mm\,s^{-1}$), there is significant convective mixing in the receiving stream. Also, because active flow is maintained in the receiving channel, the reactants are transported while they react, which means that the flow axis is linearly related to time of reaction, so that kinetics may be monitored directly by spatial imaging.

To test these ideas, confocal fluorescence microscopy was used to study mixing and reaction in a two-layer structure coupled by a nanocapillary array membrane (inset Figure 1c and Supporting Information) under conditions in which the receiving channel flow was maintained. The capacity of these structures to achieve rapid mixing was initially tested by injecting 2 μM fluorescein in phosphate buffer from a source channel into a receiving channel that contained only buffer (Figure 1a). The source channel solution emerges from individual nanopores and is mixed (diluted) in a volume whose lateral dimensions are determined by the interpore spacing. Under $1\,mm\,s^{-1}$ flow velocities cross-sectional fluorescence imaging indicates that complete mixing, both laterally and in depth, is achieved within the first half of the channel overlap region (45 μm, position 3 of Figure 1a), consistent with the simple estimate above.

Since rapid mixing is observed, it is natural to ask whether these structures can be used for kinetic studies of reactions in which the reagent amounts preclude bench-scale studies. Derivatization of glycine with *o*-phthaldialdehyde (OPA) and 2-mercaptoethanol (ME) was used to test this possibility. The

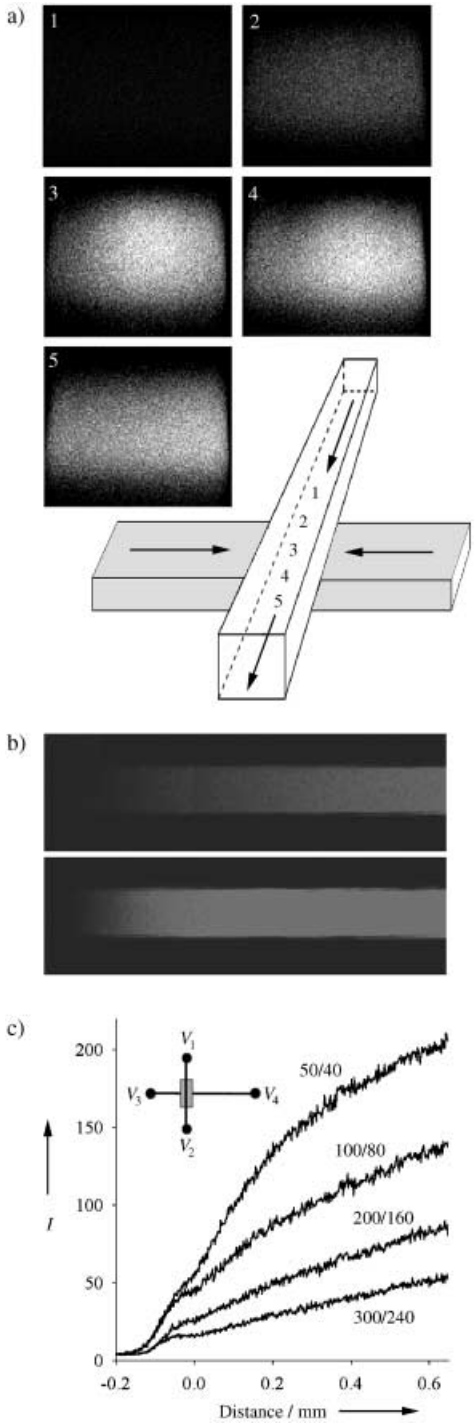

Figure 1. a) Cross-sectional fluorescence images normal to the flow axis at positions upstream (1) through to downstream (5), of the 90 μm wide nanocapillary array intersection. The fluorescein solution in the horizontal channel was injected through the nanocapillary array into the receiving (observation) channel. Positions (2), (3), and (4) are at the upstream edge, in the middle, and at the downstream edge of the intersection, respectively. b) Fluorescence images of the reaction of glycine with OPA/ME as a function of distance along the receiving channel with $V_1 = V_2$ and $V4 = 0$; V_n is the voltage applied in the respective reservoirs. Top, fast-channel flow $\{V_1,V_3\} = \{200,160\}$. Fluorescence intensity (I, arbitrary units) as a function of distance (time) in the reaction of glycine with OPA/ME along the receiving channel under applied voltages at fixed $R_v = 1.25$

reactants are nonfluorescent, but OPA reacts with primary amines in the presence of ME to form a fluorescent isoindole. Fluorescence images of the reaction of glycine with OPA/ME as a function of distance along the receiving channel are shown in Figure 1b. The reaction time within the observation window was varied by controlling the ratio, $R_V = V_1/V_3$, of the potential controlling forward bias, $V_1 = V_2$, to that controlling the flow rate in the receiving channel, V_3 ($V_4 = 0$). As indicated in the inset of Figure 1c, V_1 and V_2 are the voltages applied to the respective source reservoirs and V_3, V_4 for the receiving channel. In all cases, the flow direction is from the source channel into the receiving channel towards the waste (V_4) reservoir when forward bias is applied. All data shown are for fluorescence detection in the receiving channel. It is immediately evident from Figure 1b that the reaction proceeds further towards completion within the observation window under low-voltage conditions (slow flow rate) than at high-voltage conditions (fast flow rate). A variation of R_V shows that optimum reaction kinetics are achieved at an intermediate R_V, thus indicating a trade-off between delivery of sufficient reagent to saturate the second-order reaction and making the forward bias potential so high that backflow is observed. At a fixed R_V the reaction can be observed at various flow rates, Figure 1c, and the experimental data fit to a model which depends on the flow rate ($\propto V_3$) and the reaction rate. As detailed in the Supporting Information, the time constant for the reaction to reach steady state is independent of flow rate, as expected, and gives a second-order rate constant $530 \pm 40\,\text{M}^{-1}\text{s}^{-1}$ for the reaction of OPA/ME adduct with glycine. This result agrees with the reported value after the OPA/ME equilibrium and amine group dissociation are included.[26] We note that the nanofluidically gated microfluidic scheme presented here is well-suited to screening of combinatorial chemistry products because it allows product formation to be followed in real time for sequential reactions on the same target under identical experimental conditions.

Ca^{2+} ion binding to calcium green-labeled dextrans (CGD) was also studied in the presence of ethylene glycol-bis(2-aminoethylether)-*N*,*N*,*N*,*N*-tetraacetic acid (EGTA). The modest fluorescence of native CGD increases drastically when it binds Ca^{2+} ions. Fluorescence microscopy, Figure 2a, shows that the low background fluorescence in the receiving channel increases dramatically when Ca^{2+} ions are injected through the nanocapillary array. Monitoring of the change in fluorescence intensity at a single position enables metal-ion sensing as shown in Figure 2b and c. The series of injections detected at the intersection in Figure 2b demonstrate the rapid approach to steady-state fluorescence of this chemical-sensing reaction and the trial-to-trial repeatability, while the concentration response is shown in Figure 2c. The rapid mixing utilizing the nanofluidic membrane is a key for fast chemical sensing. In applications in which the nanofluidic membrane injection is to be used for chemical sensing, the mass-transfer efficiency of the membrane is of interest. Previous work in this laboratory has shown that under the right operating conditions, 100% mass-transfer efficiency can be achieved,[24] which means that the reactive coupling through nanocapillary arrays can be used quantitatively.

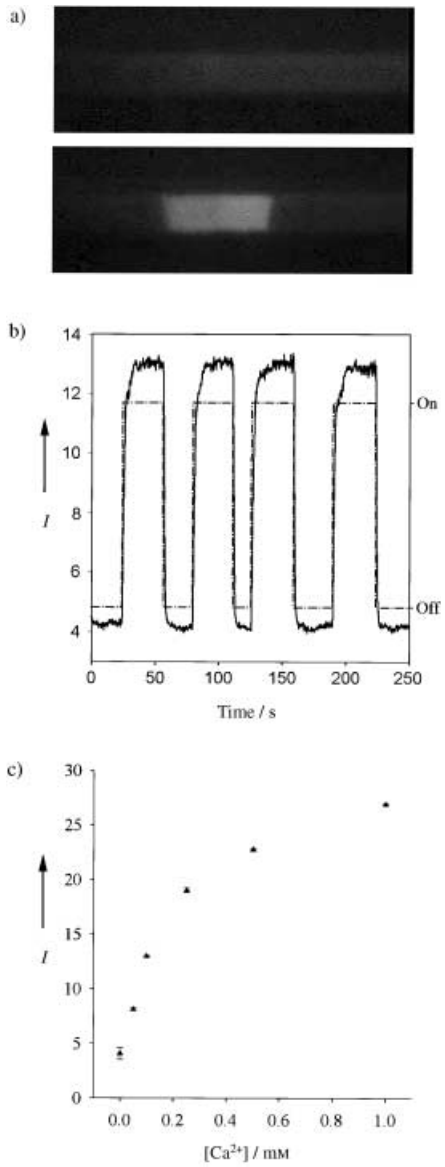

Figure 2. a) Fluorescence images of Ca^{2+}–CGD binding reaction. Top: membrane reverse bias; bottom: membrane forward bias. Ca^{2+} is injected into the horizontal CGD channel. b) Fluorescence intensity (*I*, left ordinate) and applied bias state (right ordinate, ----) as a function of time, which shows the transport of Ca^{2+} ions across a nanocapillary array (pore diameter 200 nm) to the CGD-containing channel (2 μM). c) Fluorescence intensity of Ca^{2+}–CGD in the receiving channel as a function of $[Ca^{2+}]$.

A number of interesting problems are sample-limited, either due to the danger of acquiring samples, for example, biotoxins, or inherent sample size limitations, for example, single subcellular organelles. The capacity of the hybrid nanocapillary/microchannel architectures to serve as efficient, externally gatable microreactors promises to open the full armamentarium of chemical reactivity studies to mass-limited samples. By simple manipulation of the physical design of the nanofluidic interconnect control can be exerted over the spatial and temporal characteristics, for example, mixing ratio, of analytes and solvents between microfluidic channels. Compared to other mixer designs, it is simple and

versatile. The Ca^{2+} ion detection is proof-of-concept in using the nanocapillary-mixer construct for microsensing, a result which we are currently extending to other sensing schemes for metals and volatile organics.

Received: November 7, 2003
Revised: December 18, 2003 [Z53279]

Keywords: fluorescent probes · kinetics · microreactors · nanostructures · sensors

[1] S. C. Terry, J. H. Jerman, J. B. Angell, *IEEE Trans. Electron Devices* **1979**, *26*, 1880.
[2] A. Manz, N. Graber, H. M. Widmer, *Sens. Actuators B* **1990**, *1*, 244.
[3] G. J. M. Bruin, *Electrophoresis* **2000**, *21*, 3931.
[4] D. J. Beebe, G. A. Mensing, G. M. Walker, *Annu. Rev. Biomed. Eng.* **2002**, *4*, 261.
[5] D. R. Reyes, D. Iossifidis, P. A. Auroux, A. Manz, *Anal. Chem.* **2002**, *74*, 2623.
[6] P. A. Auroux, D. Iossifidis, D. R. Reyes, A. Manz, *Anal. Chem.* **2002**, *74*, 2637.
[7] C.-K. Chan, Y. Hu, S. Takahashi, D. L. Rousseau, W. A. Eaton, J. Hofrichter, *Proc. Natl. Acad. Sci. USA* **1997**, *94*, 1779.
[8] J. B. Knight, A. Vishwanath, J. P. Brody, R. H. Austin, *Phys. Rev. Lett.* **1998**, *80*, 3863.
[9] S. Böhm, K. Greiner, S. Schlautmann, S. de Vries, A. van den Berg in *Micro Total Analysis Systems 2001* (Eds.: J. M. Ramsey, A. van den Berg), Kluwer, Monterey, CA, USA, **2001**, pp. 25.
[10] L.-H. Lu, K. S. Ryu, C. Liu in *Micro Total AnalysisSystems 2001* (Eds.: J. M. Ramsey, A. van den Berg), Kluwer, Monterey, CA, USA, **2001**, pp. 28.
[11] D. B. Beebe, G. Mensing, J. Moorthy, C. Khoury, T. Pearce, in *Micro Total Analysis Systems 2001* (Eds.: J. M. Ramsey, A. van den Berg), Kluwer Academic Publishers, Monterey, CA, USA, **2001**, pp. 453.
[12] J. Choi, C. Hong, C. Ahn in *Micro Total AnalysisSystems 2001* (Eds.: J. M. Ramsey, A. van den Berg), Kluwer, Monterey, CA, USA, **2001**, p. 621 – 622.
[13] M. Oddy, J. Santiago, J. Mikkelsen, *Anal. Chem.* **2002**, *74*, 5822.
[14] Z. Yang, H. Goto, M. Matsumoto, R. Maeda, *Electrophoresis* **2000**, *21*, 116.
[15] F. G. Bessoth, A. J. deMello, A. Manz, *Anal. Commun.* **1999**, *36*, 213.
[16] J. P. Kutter, S. C. Jacobson, J. M. Ramsey, *Anal. Chem.* **1997**, *69*, 5165.
[17] A. D. Stroock, S. K. W. Dertinger, A. Ajdari, I. Mezić, H. A. Stone, G. M. Whitesides, *Science* **2002**, *295*, 647.
[18] M. Elwenspoek, T. S. J. Lammerink, R. Miyake, J. H. J. Fluitman, *J. Micromech. Microeng.* **1994**, *4*, 227.
[19] G. H. Seong, R. M. Crooks, *J. Am. Chem. Soc.* **2002**, *124*, 13360.
[20] R. F. Ismagilov, J. M. K. Ng, P. J. A. Kenis, G. M. Whitesides, *Anal. Chem.* **2001**, *73*, 5207.
[21] J. Dai, T. Ito, L. Sun, R. W. Crooks, *J. Am. Chem. Soc.* **2003**, *125*, 10.1021/ja0374776.
[22] Y. Zhang, A. T. Timperman, *Analyst* **2003**, *128*, 537.
[23] T.-C. Kuo, D. M. Cannon, Jr., W. Feng, M. A. Shannon, J. V. Sweedler, P. W. Bohn, *Anal. Chem.* **2003**, *75*, 1861.
[24] T.-C. Kuo, D. M. Cannon, Jr., M. A. Shannon, P. W. Bohn, J. V. Sweedler, *Sens. Actuators A* **2003**, *102*, 223.
[25] D. M. Cannon, Jr., T.-C. Kuo, J. V. Sweedler, P. W. Bohn, *Anal. Chem.* **2003**, *75*, 2224.
[26] E. Trepman, R. F. Chen, *Arch. Biochem. Biophys.* **1980**, *204*, 524.

